15th Triennial World Congress, Barcelona, Spain

ROBUST CONTROL OF A 2D ACOUSTIC DUCT

Hemanshu R. Pota [**,1] **Ian R. Petersen** [**,1] **Atul G. Kelkar** [*,2]

[*] *Department of Mechanical Engineering, Iowa State University, Ames IA 50011 USA, Telephone: 515 2940788, Email: akelkar@iastate.edu*
[**] *School of Electrical Engineering, UNSW at the Australian Defence Force Academy, Canberra ACT, 2600, Australia. Telephone: +61 2 62688193, Fax: +61 2 62688443, Email: {hrp,irp}@ee.adfa.edu.au.*

Abstract: This paper reports the experimental results in the application of feedback control of acoustic noise in a 2D duct. It is shown that the feedback control of 2D ducts poses peculiar problems compared to simple 1D ducts. The chief amongst them are the need for explicit budgeting of uncertainties and dealing with high model orders. This paper demostrates a practical way to design controllers for such systems using minimax LQG methods. It is shown that an important step in the controller design is the proper choice of a weighting function. The results presented in this paper are impressive and they can be further improved by proper choice of actuator and sensor placements.

Keywords: Active noise control, robust control, minimax LQG control, acoustic duct, system identification, uncertainty modelling, two-dimensional duct.

1. INTRODUCTION

Active reduction or control of acoustic noise has significant practical applications (Elliott, 1999). Successful active noise control schemes mostly use adaptive feedforward control (Elliott, 1999; Hu *et al.*, 1998; Omoto and Elliott, 1999). Feedforward control is ideal in the situations where a signal strongly correlated with the noise can be directly measured. There are many practical applications, e.g., structure induced vibrations, where it's difficult to obtain an acoustic noise correlated signal which can be used to effect a feedforward control scheme. In these situations it's fruitful to apply feedback control for active noise reduction.

The essentials of modelling and control of a 1D duct have been discussed in (Pota and Kelkar, 2001; Kelkar and Pota, 2000). Experimental results using feedback have been obtained for 1D ducts; see (Hong *et al.*, 1996; Clark and Cole, 1995) for results without robust control approach whilst the work in (Kelkar and Pota, 2000; Erwin and Bernstein, 1997; Petersen and Pota, 2000; Petersen, 2001) uses robust control theory to design controllers. It is well-known (Pota and Kelkar, 2000) that for feedforward control a perfect model matching is essential to provide satisfactory noise cancellation. In feedback control, a mismatch in model can lead to an unstable system. This is the main reason for the reluctance to use feedback control for acoustic noise reduction. This means that the proper use of robust control theory is essential to obtain results which have practical applications. For example, the significant improvement of feedback controller performance in (Petersen and Pota, 2000) over the other reported feedback controllers is due to its explicit accounting of modelling uncertainties.

All the results in the literature using feedback control (Hong *et al.*, 1996; Clark and Cole, 1995; Kelkar and Pota, 2000; Petersen and Pota, 2000) are reported for 1D ducts only. In principle, conrol of 1D ducts is no different from 2D ducts. But in practice there is much difference. Firstly it's a lot easier to get excellent match between identified models and experimental data for 1D ducts. Secondly the model order of 1D ducts is significantly lower. In this paper the practical aspects of noise reduction in 2D ducts are highlighted based on experimental results. The minimax LQG feedback control (Petersen *et al.*, 2000; Ugrinovskii and Petersen, 1998)

[1] Supported by the Australian Research Council
[2] Supported by the NSF through Grant No. CMS:9713846, and NASA through Grant No. NAG-1-01039

Fig. 1. The Experimental 2D Duct

is used to design practical controllers for a 2D acoustic duct at the Iowa State University (ISU) shown in Figure 1.

2. EXPERIMENTAL SETUP AND MODELING

2.1 *Experimental Setup*

The experimental acoustic duct to be considered in this paper is shown in Figure 1. The duct is constructed from almumium sheets. One side of the duct (with the largest cross-section) has two doors on hinges which provide access to the inside of the duct to position the microphones. The experiment is so set that there are two speakers and one microphone. One speaker is used as a disturbance and the other speaker is the control speaker. There is one microphone to sense the acoustic disturbance and provide the feedback to the controller. The feedback control system is a SISO system with the disturbance coming from an independent speaker located on one end of the duct.

The 2D duct is 1850 *mm* $\times$ 1240 *mm* $\times$ 250 *mm*. Let the origin $(0,0,0)$ be at the bottom left corner when one is facing the door side of the duct; *z*-axis is up, *y*-axis is into the duct, and the *x*-axis is along the length of the duct. The disturbance speaker is located at one end of the duct with the centre at $(0,127,406)$ *mm*; the control speaker is located at $(600,430,320)$ *mm*; and the microphone is located at $(588,20,42)$ *mm*.

2.2 *System Identification and Nominal Modeling*

To identify the system model, two separate frequency responses are recorded using Stanford Research's SR785 spectrum analyser. One response from the disturbance speaker to the microphone and the other from the control speaker to the same microphone. The subspace identification technique (McKelvey *et al.*, 1996) is then used to get a state-space representation of this two-input-one-output system.

Experimental frequency response data was collected from 20–500 Hz. It is not practical to fit a model over the

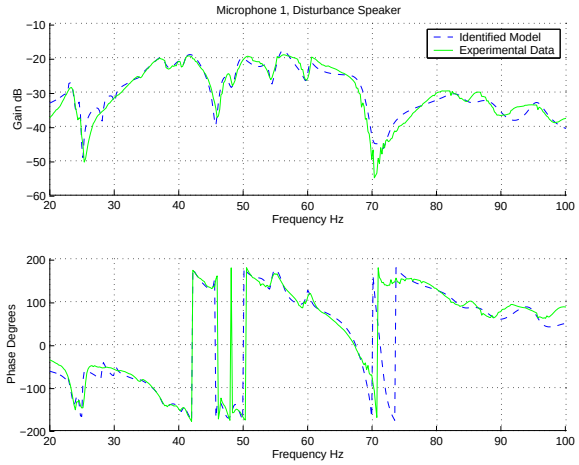

Fig. 2. Experimental and Identified Disturbance Speaker Response

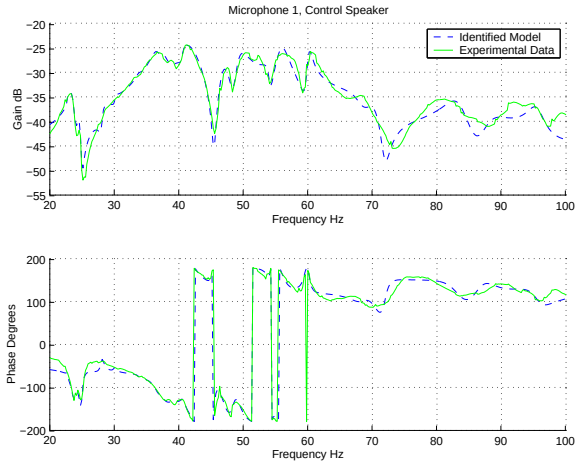

Fig. 3. Experimental and Identified Control Speaker Response

entire frequency range. A 40^{th} order model was fitted in the 20–100 Hz frequency range. Figures 2 and 3 show the experimental response and the identified response for the disturbance and control speakers, respectively. From the figures it can be seen that even a 40^{th} order model is unable to match the data exactly.

After the identification process, we end up with a nominal transfer function matrix of the form

$$P(s) = \begin{bmatrix} P_1(s) & P_2(s) \end{bmatrix}$$

where $P_1(s)$ represents the transfer function from the disturbance speaker input to the microphone output and $P_2(s)$ represents the transfer function from the control speaker input to the microphone output.

2.3 *Uncertainty Modeling*

The system representation which forms the starting point in the minimax LQG controller design is shown in Figure 4. In the figure y is the microphone output, u is the control speaker input, $\tilde{w}$ represents the noise input and it is assumed that the effects of the uncertainty show up at the sensor

output through the disturbance channel. This is one particular uncertainty model but the minimax LQG method is not restricted to this model alone and alternative representations are possible.

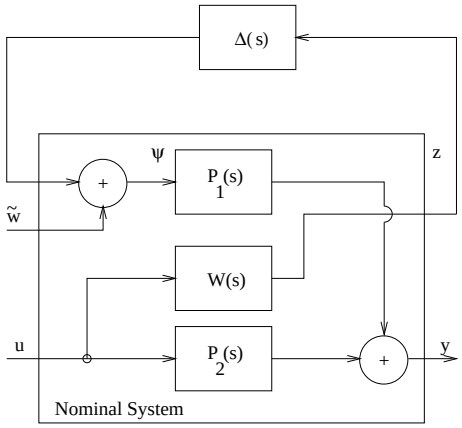

Fig. 4. Uncertain system representation.

The block $\Delta(s)$ in Figure 4 is chosen such that

$$|\Delta(j\omega)| \leq 1 \ \ \forall \ \ \omega, \tag{1}$$

and $W(s)$ is a stable frequency weighting transfer function. The controller design section will discuss the importance of choosing this weighting function properly.

Let the true transfer function from the control speaker to the microphone be given by $\tilde{P}_2(s)$. From the block diagram in Figure 4 it can be seen that

$$(\tilde{P}_2(s) - P_2(s))/P_1(s) = \Delta(s)W(s).$$

To restrict $|\Delta(j\omega)| \leq 1 \ \ \forall \ \ \omega$, the weighting function needs to be chosen such that

$$\left| \frac{\tilde{P}_2(j\omega) - P_2(j\omega)}{P_1(j\omega)} \right| \leq |W(j\omega)| \ \ \forall \ \ \omega. \tag{2}$$

The bound (2) is an inequality bound on the magnitude of $W(s)$ and there are several functions which will satisfy this bound. In this paper the function on the left-hand-side of the bound (2) is computed in the frequency range of interest from the experimental measurements and the indentified system models. From these functions a magnitude envelope is constructed and finally that magnitude envelope is matched by a transfer function obtained using the Yule-Walker method (Friedlander and Porat, 1984; Petersen *et al.*, 2002). The envelope and the magnitude of the 40^{th} order transfer function, for the identified models in Figures 2 and 3, derived using Yule-Walker method is shown in Figure 5.

3. MINIMAX LQG CONTROL

This section presents a brief description of the minimax LQG robust controller synthesis method. A more complete and rigorous description of this method can be found in the references (Ugrinovskii and Petersen, 1998; Petersen *et al.*, 2000). The minimax LQG method is applied to uncertain systems of the form shown in Figure 6. In this

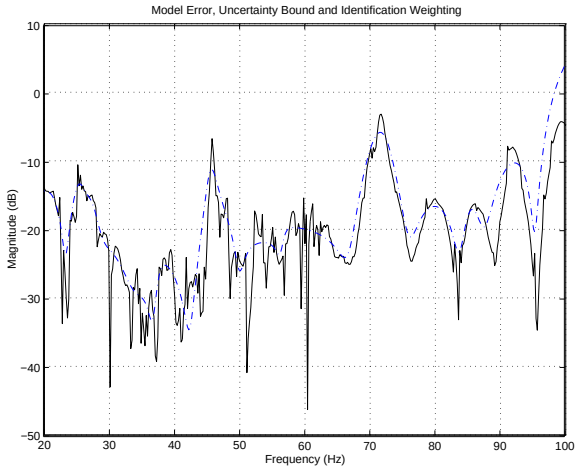

Fig. 5. Uncertainty Bound (dashed-$20\log 10|W(j\omega)|$, solid-$20\log 10|\tilde{P}_2(j\omega) - P_2(j\omega)|/||P_1(j\omega)|$)

figure, the nominal system is described by the following stochastic state equations:

$$\begin{aligned} \dot{x} &= (Ax + B_1 u + B_2\phi) + B_2\tilde{w}, \\ z &= C_1 x + D_1 u, \\ y &= C_2 x + D_2\phi + D_2\tilde{w}, \quad y(0) = 0, \end{aligned} \tag{3}$$

In the above equations, $x(t) \in \mathbf{R}^n$ is the state, $u(t) \in \mathbf{R}^m$ is the control input, $\tilde{w}(t)$ is a unity covariance white noise input, $z(t) \in \mathbf{R}^q$ is the uncertainty output, $\phi(t) \in \mathbf{R}^p$ is the uncertainty input and $y(t) \in \mathbf{R}^l$ is the measured output.

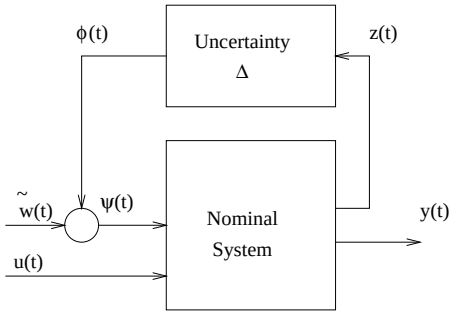

Fig. 6. Stochastic uncertain system.

The uncertainty block can be any dynamical system satisfying a general uncertainty constraint; see (Petersen *et al.*, 2000; Ugrinovskii and Petersen, 1998). In particular, this uncertainty constraint is satisfied by the uncertainty block $\Delta(s)$ in equation (1).

It is assumed that the cost function under consideration is of the form (**E**(.) is the expected value)

$$J = \lim_{T\to\infty} \frac{1}{2T}\mathbf{E}\int_0^T (x(t)'Rx(t) + u(t)'Gu(t))dt, \tag{4}$$

where $R \geq 0$ and $G > 0$. The minimax LQG control problem involves finding a controller which minimises the maximum of this cost function where the maximum is taken over all uncertainties satisfying the uncertainty constraint (1). If we define a variable

$$\zeta = \begin{bmatrix} R^{\frac{1}{2}}x \\ G^{\frac{1}{2}}u \end{bmatrix}, \tag{5}$$

then the minimax LQG control problem can be solved by solving the scaled H^∞ control problem represented in Figure 7; see (Petersen *et al.*, 2000; Ugrinovskii and Petersen, 1998).

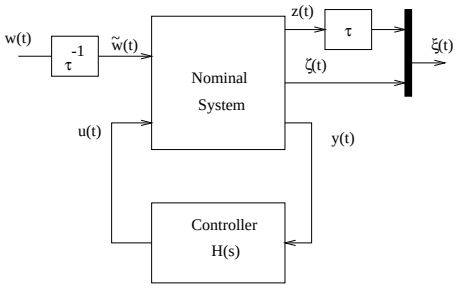

Fig. 7. The scaled H^∞ control problem.

In this H^∞ control problem, the nominal system is described by equations (3) and (5) and the controller is to be constructed such that the closed loop system is stable and the transfer function from $\tilde{w}(t)$ to $\xi(t)$ satisfies the H^∞ norm bound

$$\|T_{\tilde{w}\xi}(j\omega)\| \leq 1 \ \ \forall \omega.$$

It is well known that the solution to this H^∞ control problem can be obtained in terms of the following pair algebraic Riccati equations (e.g., see (Zhou *et al.*, 1996)):

$$\begin{aligned}
&(A - B_2 D_2'(D_2 D_2')^{-1} C_2) Y_\infty \\
&+ Y_\infty (A - B_2 D_2'(D_2 D_2')^{-1} C_2)' \\
&- Y_\infty (C_2'(D_2 D_2')^{-1} C_2 - \frac{1}{\tau} R_\tau) Y_\infty \\
&+ B_2 (I - D_2'(D_2 D_2')^{-1} D_2) B_2' = 0
\end{aligned} \tag{6}$$

and

$$\begin{aligned}
&X_\infty (A - B_1 G_\tau^{-1} \Upsilon_\tau') + (A - B_1 G_\tau^{-1} \Upsilon_\tau')' X_\infty \\
&+ (R_\tau - \Upsilon_\tau G_\tau^{-1} \Upsilon_\tau') \\
&- X_\infty (B_1 G_\tau^{-1} B_1' - \frac{1}{\tau} B_2 B_2') X_\infty = 0,
\end{aligned} \tag{7}$$

where the solutions are required to satisfy the conditions $Y_\infty > 0$, $X_\infty > 0$, $I - \frac{1}{\tau} Y_\infty X_\infty > 0$ and $R_\tau - \Upsilon_\tau' G_\tau^{-1} \Upsilon_\tau \geq 0$. Here $R_\tau \triangleq R + \tau C_1' C_1$, $G_\tau \triangleq G + \tau D_1' D_1$ and $\Upsilon_\tau \triangleq \tau C_1' D_1$. In order to solve the minimax LQG control problem, the parameter $\tau > 0$ is chosen to minimize the cost bound W_τ (the upperbound on J in (4)) defined by

$$W_\tau \triangleq \text{tr} \begin{bmatrix} (\tau Y C_2^T + B_2 D_2^T)(D_2 D_2^T)^{-1} \\ \times (\tau C_2 Y + D_2 B_2^T) X (I - YX)^{-1} \\ + \tau Y R_\tau \end{bmatrix}. \tag{8}$$

Then, the minimax LQG controller is defined by the state equations

$$\begin{aligned}
\dot{\hat{x}} &= (A - B_1 G_\tau^{-1} \Upsilon_\tau') \hat{x} \\
&\quad - (B_1 G_\tau^{-1} B_1' - \frac{1}{\tau} B_2 B_2') X_\infty) \hat{x} \\
&\quad + (I - \frac{1}{\tau} Y_\infty X_\infty)^{-1} (Y_\infty C_2' + B_2 D_2') \\
&\quad \times (D_2 D_2')^{-1} \left(y - (C_2 + \frac{1}{\tau} D_2 B_2' X_\infty) \hat{x} \right) \\
u_\tau &= -G_\tau^{-1} (B_1' X_\infty + \Upsilon_\tau') \hat{x}.
\end{aligned} \tag{9}$$

4. CONTROLLER DESIGN

The appropriate state-space representaton in equation (3) are arrived at from $P_1(s)$, $P_2(s)$, and $W(s)$ as discussed previously. Note that the theory of (Ugrinovskii and Petersen, 1998; Petersen *et al.*, 2000) requires that $D_2 D_2' > 0$ in (3). This is achieved by adding a small measurement noise to the system in addition to the process noise $\tilde{w}(t)$. We choose the matrix R in the cost function (4) as $R = C_2' C_2$. That is, the term $x(t)' R x(t)$ in the cost function (4) corresponds to the norm squared value of the nominal system output. The term $u' G u$ in the cost function (4) is treated as a design parameter affecting controller gain. However, in all cases it was found that setting G to the small value of $G = 10^{-8}$ did not lead to excessive controller gains.

Note that with the above choice of plant model (3) and cost function (4), the nominal LQG problem essentially amounts to the problem of minimizing the noise energy at the microphone position when the system is subject to a white noise disturbance entering the system through the control input channel.

The minimax LQG controller is synthesized by first choosing the constant $\tau > 0$ to minimize the quantity W_τ defined in (8). With this value of the parameter τ, the controller is constructed according to the formula (9). The order of this controller will be the sum of the order of the nominal plant model $P(s)$ together with the order of the weighting filter $W(s)$. For the case under discussion the controller order is 80. Such a high order controller may lead to problems of numerical error and excessive computational load when implemented. Hence, the balanced controller reduction method described in Section 19.1.1 of (Zhou *et al.*, 1996) was applied in order to obtain a 40th order approximation to the 80th order controller. It was found that with this level approximation, there was very little degradation in the predicted closed loop performance. The designed controller is shown in Figure 8.

5. EXPERIMENTAL RESULTS

The reduced dimension controller designed in Section 4 was implemented on a dSPACE DS1103 system as shown in Figure 9. The spectrum analyser is used to measure the closed loop frequency response from the disturbance speaker input to the microphone output. In order to implement each controller, it was first discretized using the FOH method with a sample period of 0.5×10^{-3} seconds. The resulting discrete

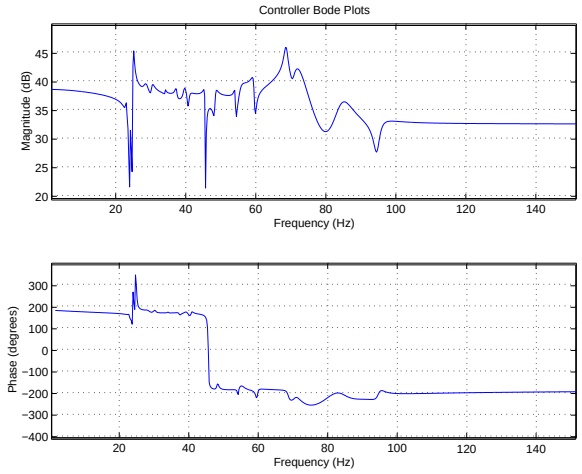

Fig. 8. LQG minimax Controller

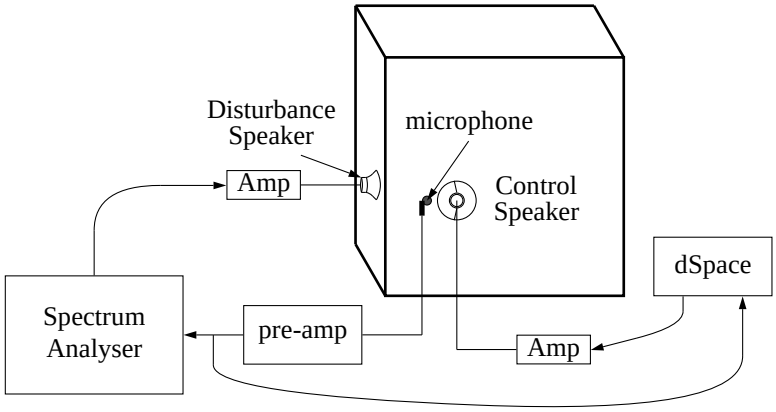

Fig. 9. Two dimensional duct feedback controller setup

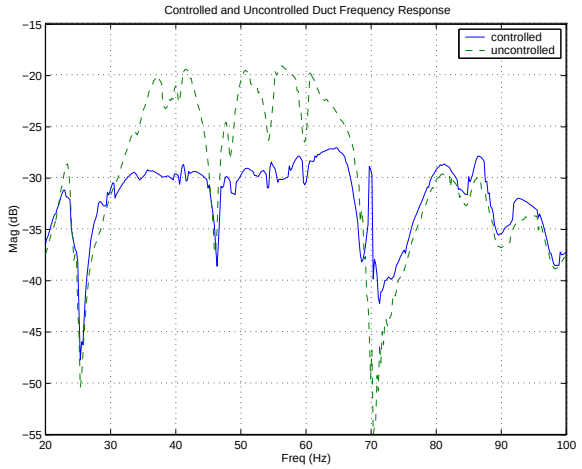

Fig. 10. Experimental Closed Loop and Open Loop Response

time controller was then implemented on the dSPACE system with this sample period. Figure 10 shows the resulting measured frequency response for the open loop and closed loop system.

6. PROPER CHOICE OF THE UNCERTAINTY MODEL

In the closed loop response in Figure 10 it can be seen that there is an increase in the gain near the deep null around

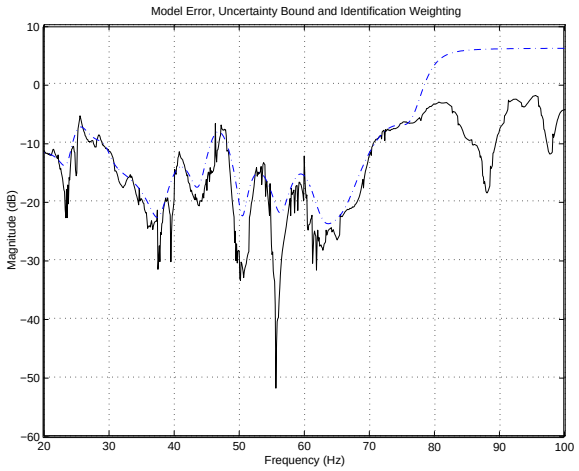

Fig. 11. Uncertainty Bound (dashed-$20\log10|W(j\omega)|$, solid-$20\log10|\tilde{P}_2(j\omega) - P_2(j\omega)|/|P_1(j\omega)|$)

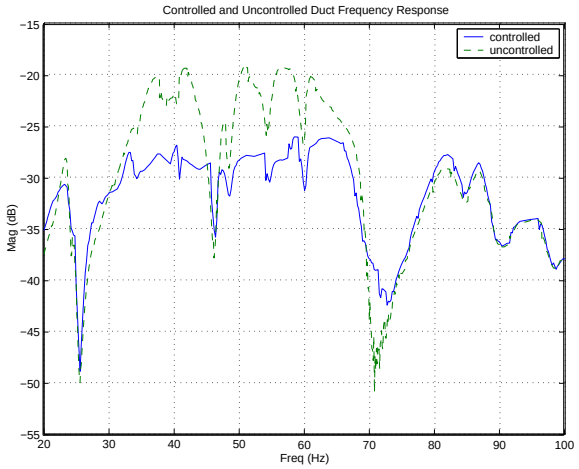

Fig. 12. Experimental Closed Loop and Open Loop Response

70 Hz. This is due the extreme difficulty in finding a good match between the identified model and the experimental data. To shape the closed loop response at 70 Hz the choice of frequency weighting function $W(s)$ is slightly altered as shown in Figure 11. The envelope is chosen very conservatively at frequencies greater than 70 Hz. The experimental response of the controller designed with this method is shown in Figure 12. From the figure it's clear that a proper selection of the weighting function helps in shaping the closed loop response.

7. CONTROL OF HIGHER FREQUENCY MODES

The experimental results presented thus far were restricted to the lower frequency range of 20–100 Hz. In this section the minimax LQG control method is used to demonstrate the controller performace between 250–450 Hz. The choice of uncertainty envelope and the experimental closed loop and open loop performace is shown in Figures 13 and 14, respectively. There is a clear improvement in the damping of the resonant peaks in the frequency range of interest.

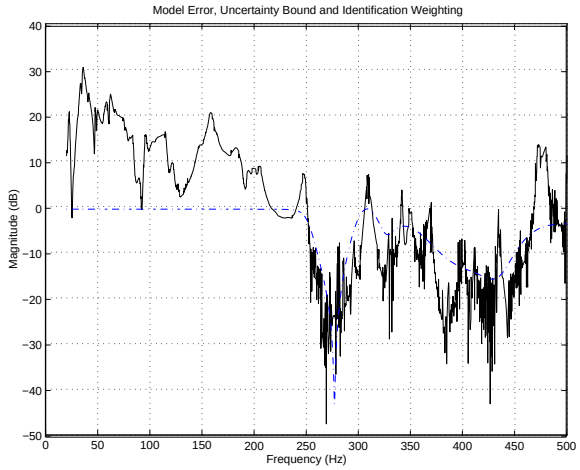

Fig. 13. Uncertainty Bound (dashed-$20\log 10|W(j\omega)|$, solid-$20\log 10|\tilde{P}_2(j\omega) - P_2(j\omega)|/|P_1(j\omega)|$)

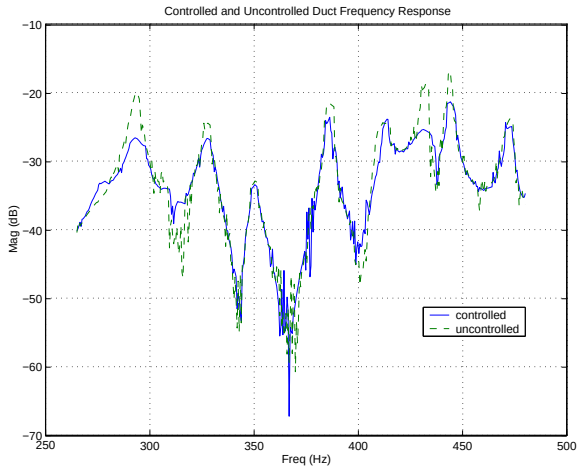

Fig. 14. Experimental Open Loop and Closed Loop Response

8. CONCLUSIONS

This paper successfully demonstrates that feedback control can be applied to very high order acoustical systems. Due to the practical difficulty in implementing very high order controllers it is essential that a small frequency band be selected for noise attenuation. The chosen minimax LQG control method gives the flexibility to choose the frequency weighting function $W(s)$ such that the controller targets a specified frequency band. Overall the experimental results in this work are very impressive and further work in the selection of actuator-sensor placement (to obtain a tighter fit between the model and data) and a choice of frequency weighting function can improve the results significantly.

9. REFERENCES

Clark, R. L. and D. G. Cole (1995). Active damping of enclosed sound fields through direct rate feedback control. *J. of Acoustic Society of America* **97**(3), 1710–1716.

Elliott, Stephen J. (1999). Down with noise. *IEEE Spectrum* pp. 54–61.

Erwin, R. Scott and Dennis S. Bernstein (1997). Discrete-time h_2/h_∞ control of an acoustic duct: Delta-domain design and experimental results. In: *Conference on Decision and Control*. IEEE. San Deigo, CA. pp. 281–282.

Friedlander, B. and B. Porat (1984). The modified yule-walker method of arma spectral estimation. *IEEE Transactions on Aerospace Electronic Systems* **20**(2), 158–173.

Hong, Jeongho, James C. Akers, Ravinder Venugopal, Miin-Nan Lee, Andrew G. Sparks, Peter D. Washabaugh and Dennis S. Bernstein (1996). Modeling, identification, and feedback control of noise in an acoustic duct. *IEEE Transactions on Control Systems Technology* **4**(3), 283–291.

Hu, Jwu-Sheng, Shiang-Hwua Yu and Cheng-Shiang Hsieh (1998). Application of model-matching techniques to feedforward active noise control design. *IEEE Transactions on Control Systems Technology* **6**(1), 33–42.

Kelkar, A. G. and H. R. Pota (2000). Robust broadband control of acoustic duct. In: *Proceedings of the 39th IEEE Conference on Decision and Control*. Sydney, Australia. pp. 4485–4490.

McKelvey, T., H. Akçay and L. Ljung (1996). Subspace-based multivariable system identification from frequency response data. *IEEE Transactions on Automatic Control* **41**(7), 960–979.

Omoto, Akira and Stephen J. Elliott (1999). The effect of structured uncertainty in the acoustic plant on multichannel feedforward control systems. *IEEE Transactions on Speech and Audio Processing* **7**(2), 204–212.

Petersen, I. R. (2001). Multivariable control of noise in an acoustic duct. In: *Proceedings of the European Control Conference ECC2001*. Porto, Portugal.

Petersen, I. R. and H. R. Pota (2000). Minimax LQG optimal control of an experimental acoustic duct. In: *IEE Control 2000 Conference*. Cambridge UK.

Petersen, I. R., V. Ugrinovski and A. V. Savkin (2000). *Robust Control Design using H^∞ Methods*. Springer-Verlag. London.

Petersen, Ian R., Hemanshu R. Pota and M. Reza Sayyah Jahromi (2002). System identification, uncertainty modelling and actuator placement in the robust control of an acoustic duct. In: *Proceedings of the Conference on Information, Decision, and Control (to appear)*. Adelaide, Australia.

Pota, H. R. and A. G. Kelkar (2000). On perfect noise cancelling controllers. In: *American Control Conference*. Vol. 5. Chicago, Illinois. pp. 3018–3022.

Pota, Hemanshu R. and Atul G. Kelkar (2001). Modelling and control of acoustic ducts. *ASME Journal of Vibrations and Acoustics* **123**(1), 2–10.

Ugrinovskii, V. A. and I. R. Petersen (1998). Time-averaged robust control of stochastic partially observed uncertain systems. In: *Proceedings of the IEEE Conference on Decision and Control*. IEEE. Tampa, FL.

Zhou, Kemin, John C. Doyle and Keith Glover (1996). *Robust and Optimal Control*. Prentice Hall. NJ.